Leveraging Capacity with Energy Consumption in 4G and Beyond Refarming and Reconfiguration Scenarios

S. Henriques
Instituto Superior Técnico,
University of Lisbon
Lisbon, Portugal
sara.r.henriques@tecnico.ulisboa.pt

***Abstract*—The evolution of mobile communication technologies, associated with the emergence of 5th Generation (5G) systems, have increased the variety and quantity of functionalities provided by the wireless network, thus being one of the main contributors to global mobile traffic growth. This evolution has a major impact on Base Stations (BSs) energy consumption, along with the gradual increase of subscribers. However, traffic growth and radio capabilities are not easily predictable, requiring operators to constantly revise their planning forecasts to fulfill all Quality of Service (QoS) and Quality of Experience (QoE) requirements. The aim of this paper is to present capacity models for both 4th Generation (4G) and 5G technologies, each one for a distinct vendor, and provide energy saving scenarios in order to increase the BSs energy efficiency, using existing energy consumption models. The proposed capacity models are both based on supervised Machine Learning (ML) techniques using data collected from two real mobile network operators. This approach provides the detection of capacity saturation problems and the prediction of the maximum cell capacity, under realistic conditions. The considered scenarios are based in frequency bands and technologies switch-off techniques, combined with further analysis of both energy and capacity impact in the concerned BS.**

***Index Terms*—Mobile networks, capacity modeling, energy consumption, 4G, 5G, Machine Learning.**

I. Introduction

Nowadays, mobile traffic is escalating with the growing number of wireless users along with the increased traffic volume per subscriber, derived from advanced applications such as high-resolution video streaming, remote monitoring and real-time control applications. Mobile data traffic grew by 56% between Q1 2019 and Q1 2020 [1]. In addition to the evolution of the current mobile communication technologies, the gradual emergence of 5th Generation (5G) devices will have a strong impact on this growth. By 2025, it is estimated that 45% of total mobile data traffic will be carried by 5G networks [1].

The exponential growth of mobile data traffic requires operators to estimate the capacity of the cells, in order to guarantee an adequate Quality of Service (QoS) and Quality of Experience (QoE) for end users. Once the capacity of a cell is exceeded, these parameters reach unacceptable levels. Thus, an accurate cell capacity estimate is necessary to fulfill QoS requirements with minimal network investment [2].

This rapid evolution of mobile data consumption has led to an increase in the number of Base Stations (BSs). However, the BS is the main energy consumer in a cellular network and can reach 57% of all the mobile operator energy consumption [3]. Thus, BS energy consumption monitoring helps operators to become aware of their energy consumption, in order to assess the impact of their subsequent decisions.

To overcome these concerns, models that predict the cell capacity in both 4th Generation (4G) and 5G mobile networks are proposed in this paper, along with energy efficiency scenarios of traffic migration. The capacity models are based on real measurements, using Multiple Linear Regression (MLR) algorithms. The main advantage of these measurement-based approaches is to consider the peculiarities of each cell, such as propagation conditions, channel quality and latency. Subsequently, two traffic migration scenarios, associated with Universal Mobile Telecommunications System (UMTS) technology, are developed in order to provide energy efficiency solutions of the BSs, by using existing power consumption models for the radio equipment. Finally, a simple 5G data traffic migration scenario is added to predict the impact of 4G traffic on the resources that 5G provides.

This paper is organized as follows: in Section II the existing power consumption models are analyzed; Section III presents the 4G cell capacity model with the respective results; Section IV highlights the 5G cell capacity model and its results; Section V presents the traffic volume migration scenario through the UMTS 2100 MHz (U2100) frequency band switch-off; Section VI provides the transfer scenario with the complete 3G switch-off; Section VII addresses the simple 5G scenario of data traffic volume migration; Finally, conclusions are drawn in Section VIII.

II. Energy Consumption Prediction Model

As mentioned before, the first scenario developed in this paper uses existing multi-technology energy consumption models, presented in [4], in order to estimate the power consumption by Remote Radio Units (RRUs).

A. Methodology

Dataloggers (developed by CELFINET) were used to measure the power consumption. The power consumption of the RRUs operating on 2nd Generation (2G), 3rd Generation (3G) and 4G technologies was studied over a period of 20 days, being 11 days used for training the model and 9 days for testing it, using 20 BSs located in different cities of Portugal.

Regarding the RRUs 4G power consumption model, 90 units, operating in the frequency bands of 800 MHz, 1800 MHz and 2600 MHz, were considered; a total of 45 units operating in the 900 MHz and 2100 MHz frequency bands were monitored for the 3G technology, while 15 units were monitored for 2G technology in the frequency band of 900 MHz. In addition, 21 units shared between 2G and 3G technologies in the 900 MHz frequency band were also considered.

The proposed power consumption model for RRUs is based on network traffic statistics. Linear mixed effects models are fitted to data and the results are observed in the following.

B. Power Consumption Prediction

The proposed 4G model, formally described by (1), estimates the power consumption (in *Watt*) and was reported in [4]. In this model, β_0 is the intercept coefficient reflecting the baseline power consumption and β_1 is the coefficient associated to the traffic variable, T_{4G} (in Gb). On the other hand, β_2 and β_3 coefficients are associated with energy saving features. The model presents two levels of random variations of *intercepts*: the level 1, given by b_{0i}, representing the configurations, and level 2, with the term b_{0ij}, representing the equipment nested in the configurations. To model the error dependency, *sine* and *cosine* functions were used in the random effect term at level 2; ϵ_{ij} is the portion that is not explained by the model and assumes a distribution $\epsilon_{ij} \sim N(0, \boldsymbol{R}_{ij})$. In addition, the random effect $\boldsymbol{G}_1$ and $\boldsymbol{G}_2$ are positive-definite.

$$\begin{gathered}\boldsymbol{P}_{4G} = \beta_0 + \beta_1 \boldsymbol{T}_{4G} + \beta_2 \boldsymbol{F}_{MicroSleep} + \beta_3 \boldsymbol{F}_{Sleep} + \\ [b_{0i} + b_{0ij} + b_{1i}\boldsymbol{F}_{Sleep} + b_{1ij}\boldsymbol{F}_{Sleep} + b_{2ij}\sin(\boldsymbol{H}_{rad}) + \\ b_{3ij}\cos(\boldsymbol{H}_{rad})] + \epsilon_{ij};\ i = 1,..,8; j = 1,..,90 \\ b_i \sim N(0, \boldsymbol{G}_1); b_{ij} \sim N(0, \boldsymbol{G}_2); \epsilon_{ij} \sim N(0, \sigma_e^2 \boldsymbol{I}).\end{gathered} \tag{1}$$

Regarding the 3G model, formally described by (2), with the following independent variables: the traffic in Packet Switched (PS) Release 99 (R99), T_{R99}, the traffic in High Speed Downlink Packet Access (HSDPA), T_{HSDPA}, and the voice traffic in Circuit Switched (CS), $T_{CS_{3G}}$, all in Mb (within 15 minutes).

$$\begin{gathered}\boldsymbol{P}_{3G} = \beta_0 + \beta_1 \boldsymbol{T}_{CS_{3G}} + \beta_2 \boldsymbol{T}_{R99} + \beta_3 \boldsymbol{T}_{HSDPA} + \\ [b_{0i} + b_{0ij} + b_{1ij}\boldsymbol{T}_{HSDPA} + b_{2ij}\sin(\boldsymbol{H}_{rad}) + \\ b_{3ij}\cos(\boldsymbol{H}_{rad})] + \epsilon_{ij};\ i = 1,..,4; j = 1,..,45 \\ b_i \sim N(0, \boldsymbol{G}_1); b_{ij} \sim N(0, \boldsymbol{G}_2); \epsilon_{ij} \sim N(0, \sigma_e^2 \boldsymbol{I}).\end{gathered} \tag{2}$$

The 2G model, which is presented in (3), considered the voice traffic CS, $T_{CS_{2G}}$ in *Erlangs*, as well as the data traffic PS, $T_{PS_{3G}}$ in Mb (within 15 minutes).

$$\begin{gathered}\boldsymbol{P}_{2G} = \beta_0 + \beta_1 \boldsymbol{T}_{CS_{2G}} + \beta_2 \boldsymbol{T}_{PS_{2G}} + [b_{0i} + \\ b_{1i}\boldsymbol{T}_{CS_{2G}}] + \epsilon_i;\ i = 1,..,15; b_i \sim N(0, \boldsymbol{G}); \epsilon_i \sim N(0, \sigma_e^2 \boldsymbol{I}).\end{gathered} \tag{3}$$

Finally, the power consumption model for RRUs shared between 2G and 3G technologies is given by (4), where the same independent values of the previously presented 2G and 3G models, are used; a power function to model the error variance is also presented.

$$\begin{gathered}\boldsymbol{P}_{2G,3G} = \beta_0 + \beta_1 \boldsymbol{T}_{CS_{2G}} + \beta_2 \boldsymbol{T}_{PS_{2G}} + \beta_3 \boldsymbol{T}_{CS_{3G}} + \\ \beta_4 \boldsymbol{T}_{R99} + \beta_5 \boldsymbol{T}_{HSDPA} + [b_{0i} + b_{1i}\boldsymbol{T}_{HSDPA} + \\ b_{2i}\sin(\boldsymbol{H}_{rad}) + b_{3i}\cos(\boldsymbol{H}_{rad})] + \epsilon_i \\ i = 1,..,21; b_i \sim N(0, \boldsymbol{G}); \epsilon_i \sim N(0, \sigma_e^2 |\boldsymbol{v_i}|^{2\delta}).\end{gathered} \tag{4}$$

C. Model Results

The application of the 4G RRUs power consumption model is shown in Fig. 1, where it is possible to observe a good adjustment between estimated and measured power values. The models developed for other units have an identical behavior.

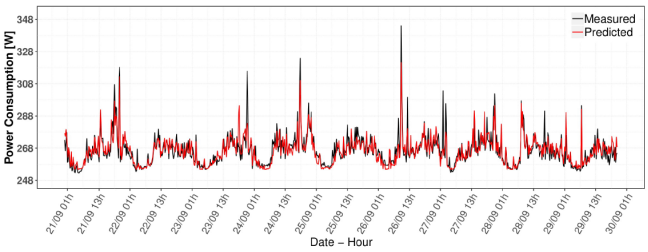

Fig. 1: 4G power consumption model prediction during 9 days [4].

The RRUs power consumption model error metrics, such as the adjusted determination coefficient R_a^2, Mean Absolute Percent Error (MAPE) and Root Mean Square Error (RMSE), are presented in Table I, for all RRUs.

TABLE I: Power consumption model error metrics [4].

Model	R_a^2	MAPE [%]	RMSE [W]
4G	0.99	1.65	6.14
3G	0.99	0.92	3.55
2G	0.88	0.38	1.04
2G/3G	0.80	1.49	6.84

III. 4G Cell Capacity Model

The aim of 4G cell capacity model is to develop cell monitoring methods to detect high load problems and to predict the maximum cell capacity on its environments, with the purpose of increasing the QoS and QoE provided by the radio network. The methodology associated with these methods was based on an existing 4G capacity model, developed for a distinct vendor and described in detail in [5].

A. Methodology

The model was developed using real network performance and configuration data collected from a Long Term Evolution (LTE) network, belonging to a Portuguese mobile operator, over a one-month period with a quarter-hourly granularity. Data were extracted from 114 cells of 22 sites, operating in the frequency bands of 800, 1800 and 2600 MHz, with system bandwidth of 10 MHz for the first frequency band, and of 20 MHz for the remaining ones. After analyzing the network data, different network scenarios were detected.

B. Cell Resource Monitoring

In this first module, information about how to locate the resource bottleneck and the related handling suggestions are provided. Downlink user perception is considered. The data traffic rise leads to an increase in the Physical Resource Block (PRB) utilization, which reflects the degree of bandwidth usage, over the air interface. On the other hand, the downlink user-perceived rate decreases as the number of users sharing the limited PRB increases, reflecting the user QoE.

The used method is based in a strategy, as in [6], although the values of each threshold were adapted to the vendor here considered, based on [7].

Thus, if the downlink PRB utilization rate reaches or exceeds 80% while the downlink user-perceived rate is below 5 Mbps for three days in a week, then the cell goes through an analysis regarding the following list of thresholds:

- Average Channel Quality Indicator (CQI) lower than 10. CQI is used by the User Equipment (UE) to indicate the channel quality to the evolved NodeB (eNB). The reported CQI value ranges from 0 to 15, indicating the type of modulation and coding that UE can operate.
- Downlink UE latency higher than 9 ms, measuring the impact on the end user. Downlink latency is a parameter that indirectly influences the perceived system data rate.
- Average 64-Quadrature Amplitude Modulation (QAM) scheme usage lower than 10%. This metric represents the percentage of 64-QAM samples, which indicates downlink Signal to Interference plus Noise Ratio (SINR) status along with CQI and Rank Indicator (RI).
- Average Radio Link Control (RLC) retransmission ratio higher than 1%. The RLC retransmission ratio can be given by the proportion of unsuccessful RLC Protocol Data Unit (PDU) and RLC PDU segment transmissions.

If all these listed conditions are fulfilled, then Radio Frequency (RF) optimization should be performed. Otherwise, it is advised to add carriers or expand the bandwidth.

In order to increase the accuracy associated with this monitoring method, only samples related to the busy hours are analyzed. Thus, as presented in Table II, 2 cells with capacity problems were detected, i.e., with a bottleneck on the downlink user perception, among the 114 existing ones.

Both cells have average CQI values below 10, therefore it is advised to perform a RF optimization (e.g. reconfiguration of antennas tilt and/or azimuth, neighboring cells, etc), minimizing the channel interference.

TABLE II: Cells detected by the resource monitoring module.

Cell	PRB Util Rate [%]	User Thp [Mbps]	Avg CQI	DL UE Lat. [ms]	Avg 64-QAM [%]	Avg RLC Retx. [%]
A	99.4	3.47	7.15	4.22	11.4	0.05
B	88.8	4.25	8.01	3.94	15.5	0.06

C. Downlink Cell Throughput Prediction

The capacity model is based on real data, using MLR algorithms to predict the downlink cell throughput. The MLR model is used to explain a response variable (dependent variable) as a linear function of several input variables (independent variables). The dataset was split in training set (around 70%) for fitting the model, and test set (30%), used to provide an unbiased evaluation of a final model fit on the training dataset. In the present model, the dependent variable is the downlink cell throughput, Thp_{cell}, in Mbps, and is given by [8]:

$$Thp_{cell} = \beta_0 + \sum_{i=1}^{n} \beta_i x_i \tag{5}$$

where β_0 is the model intercept, β_i is the coefficient of the variable x_i and n is the number of independent variables.

In the first place, it is advisable to have a wide range of variables, since it may not be obvious which variables are more important. This initial set of variables goes through a variable selection iterative process, using stepwise regression, where the most relevant describe the cell throughput. In each step, a variable is considered for addition to or subtraction from the set of explanatory variables based on some pre-specified criterion. In order to determine the model accuracy and evaluate which is the model that best fits the real data, several error metrics are used, such as the adjusted determination coefficient R_a^2, Pearson Correlation, MAPE and RMSE.

With zero intercept, the most relevant variables (x_i) that were chosen to predict the downlink cell throughput are the following:

- PRB utilization rate, in [%];
- Proportion of 64-QAM samples, in [%];
- Proportion of 16-QAM samples, in [%];
- Percentage of unsuccessful Hybrid Automatic Repeat Request (HARQ) transmissions rate using 16-QAM;
- Aggregated downlink latency for a measurement period, in [s];
- Percentage of successful RLC PDU transmissions, in [%];
- Proportion of both open and closed loop Spatial Multiplexing (SM) rank 1, regarding the Multiple-input Multiple-output (MIMO) rank distribution usage, in [%].

Analyzing Table II, cell A is detected as the worst in terms of having capacity problems and, therefore, the chosen model was built for this specific cell.

Since the purpose of creating the downlink cell throughput prediction model is to estimate the maximum cell capacity,

the samples belonging to the highest traffic periods are the most relevant for the model. Thus, in order to increase the model's accuracy, and considering that the number of samples is sufficient, only samples with PRB utilization rate values above the 70th percentile value were used.

The MLR model results are represented in Fig. 2, where it is possible to visualize both the real cell throughput, given by measurements, and the predicted one, given by the model. In order to improve the visualization of the figure, only 400 samples are displayed.

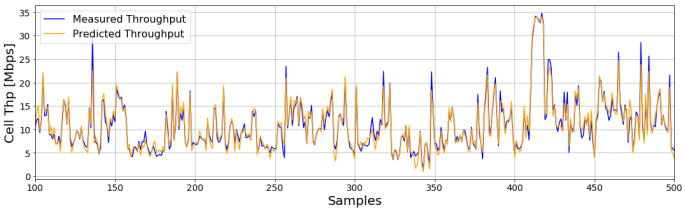

Fig. 2: Downlink cell throughput model prediction.

The model performance metrics are $R_a^2 = 0.991$, Pearson Correlation $= 97.79\%$, MAPE $= 8.91\%$ and RMSE $= 1.17$ Mbps, confirming its high reliability.

D. Cell Capacity Estimation

After the model development, it is possible to estimate the maximum cell capacity by setting the cell resources at 100%, i.e., forcing the PRB utilization rate to 100%, while the remaining variables reflect similar radio conditions.

Fig. 3 shows the measured cell throughput along with the estimated one assuming that all available PRBs are being used. In order to depict the busy hour, cell capacity and measured cell throughput are characterized by their 95th percentile values also displayed in Fig. 3.

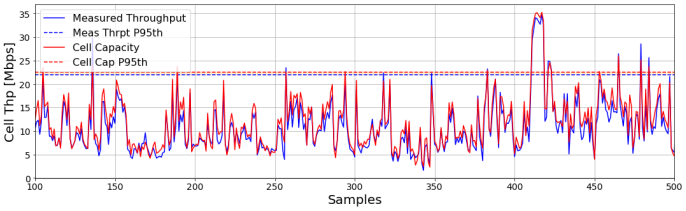

Fig. 3: 4G cell capacity estimation.

The calculated 95th percentile values of measured cell throughput and cell capacity are 21.95 Mbps and 22.52 Mbps, respectively, resulting in a cell load of 97.46%, which is consistent with the high PRB utilization rate value indicated in Table II for cell A.

E. 4G Downlink PRB Usage Prediction

In order to validate the traffic migration scenarios, a model that predicts the PRB usage is created similarly to the cell throughput prediction model, using another cell (cell C), for which the mixed effects of the power consumption model were tested, thus obtaining a more reliable prediction. In the present model, the dependent variable is the downlink PRB utilization rate, PRB_{usage}, in %, and is given by:

$$PRB_{usage} = \beta_0 + \sum_{i=1}^{n} \beta_i x_i. \quad (6)$$

The independent variables that were detected as relevant in the prediction of PRB usage rate for the four cells, with zero intercept and discarding less important variables with high Pearson Correlation (above 80%), are as follows:

- Sum of the total data traffic volume and signaling bits, in [Gb];
- Proportion of 64-QAM samples, in [%];
- Proportion of 16-QAM samples, in [%];
- Percentage of unsuccessful HARQ transmissions rate using 64-QAM, in [%].

The purpose of the current model is to estimate the PRB usage rate after migration by updating the data traffic volume variable with the new values (the old ones as well as the received volume of traffic also added), assuming the same quality of the channel.

For the current model, analogously to the first 4G capacity model, only samples with downlink cell throughput values above the 70th percentile value were used. Fig. 4 presents the proposed MLR model results, where the measured PRB usage along with the predicted one are shown.

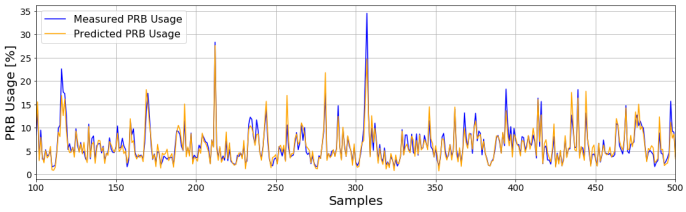

Fig. 4: 4G PRB usage model prediction.

The model performance metrics are $R_a^2 = 0.964$, Pearson Correlation $= 93.32\%$, MAPE $= 15.16\%$ and RMSE $= 1.36\%$, also confirming its high reliability.

IV. 5G Cell Capacity Model

A. Methodology

The development process of the 5G cell capacity model is similar to the one described for the 4G capacity model, regarding the mentioned methods of downlink PRB usage and downlink cell throughput prediction. However, this model uses a distinct dataset, belonging to another vendor, from a real 5G network, collected over a period of two and a half months on an hourly and cell basis. The analyzed area considers 7 cells of 3 sites, operating in the 3.5 GHz frequency band with 80 MHz of system bandwidth.

B. 5G Downlink PRB Usage Prediction

In order to estimate the downlink PRB utilization rate, in %, the dependent variable is given by:

$$PRB_{usage} = \beta_0 + \sum_{i=1}^{n} \beta_i x_i. \quad (7)$$

With zero intercept, the independent variables that were detected as the most relevant in predicting the PRB usage rate, rejecting variables with less importance and high correlation with more important variables (Pearson Correlation above 80%), are the following:

- Total downlink traffic volume in a cell, in [Gb];
- Average number of LTE-5G New Radio (NR) Non-Stand Alone (NSA) Dual Connectivity (DC) UEs using the current cell as the Primary Secondary Cell (PSCell);
- Physical Downlink Control Channel (PDCCH) Control Channel Element (CCE) usage rate, in [%];
- Average CQI values ranging from 0 to 15.

Although the majority of the 5G traffic volume is residual, since the 5G network is not yet open to public, the cell with the most data traffic was chosen; thus, the model is developed for this specific cell. However, the model's reliability will increase when more traffic has been carried on the cell.

The proposed MLR model results are presented in Fig. 5, where it is possible to visualize the measured PRB usage and the predicted by the model.

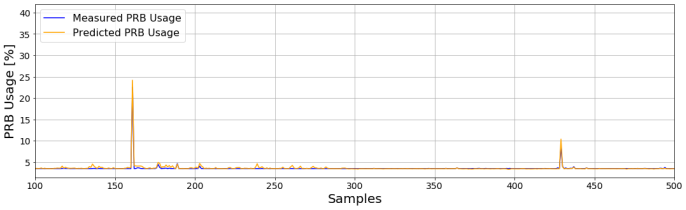

Fig. 5: 5G PRB usage model prediction.

In order to validate the model, error metrics metrics were generated: $R_a^2 = 0.990$, Pearson Correlation $= 97.35\%$, MAPE $= 2.48\%$ and RMSE $= 0.41\%$, indicating high model accuracy.

V. U2100 Traffic Migration Scenario

A. Methodology

UMTS is a legacy technology whose data traffic volume is decreasing in several operators, presenting low values in comparison to those of adjacent technologies. Therefore, in order to provide energy efficiency solutions related with the BSs, an energy saving scenario was developed, for cell C, based on traffic volume migration from U2100 frequency band, and consequently its switch-off, to other available frequency bands, whether from Global System for Mobile Communications (GSM), UMTS or LTE.

The site and sector where cell C is located was used in order to present a traffic migration scenario, consisting of a GSM 900 MHz (G900) cell, one UMTS 900 MHz (U900) cell, two U2100 cells and cell C which operates in the LTE 800 MHz (L800) frequency band. Traffic migration from all 3G cells was not considered due to the existence of a single radio shared between 2G and 3G technologies in the 900 MHz frequency band of this BS. Therefore, the traffic volume associated with the U900 band remains intact, as the radio for this frequency band cannot be switched off, since it simultaneously presents traffic volume from the G900 band.

B. Migration and Capacity Analysis

Given that the cell coverage of U900 is larger than U2100, and presupposing that this is still valid when comparing cells of different technologies, i.e., assuming that the cell coverage of L800 is also wider than U2100 in order to simplify the scenario, it is possible to transfer the voice traffic volume from the U2100 cells to the U900 cell and, in turn, their data traffic volume (PS R99 and HSDPA) to the L800 cell (cell C).

Most of the voice traffic volume is transmitted in the 2G frequency bands while, in turn, the majority of data traffic volume is transmitted in the 4G frequency bands. However, an estimation of the post-migration downlink PRB utilization rate was performed using the developed PRB usage prediction model for cell C and it is presented in Fig. 6. With migration, for the L800 cell, data traffic volume increased 30.70% while, for U900 cell, CS voice traffic increased 39.36%, both at the busy hour (within 15 minutes).

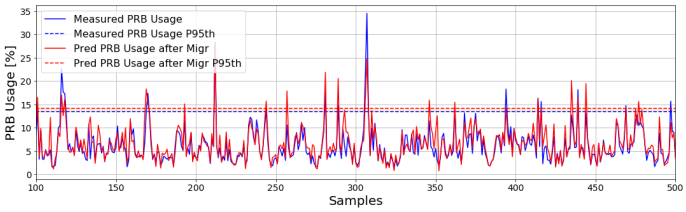

Fig. 6: 4G PRB usage prediction after traffic migration.

During the busy hour of the estimated period, the L800 cell PRB usage rate have increased nearly 4.90%, confirming that the transfer of data traffic from the U2100 cell to the L800 cell does not have a relevant impact on the PRB utilization rate of the latter. In addition, the predicted values never exceed a 100% usage rate, thus allowing its migration.

C. Energy Balance

It is also important to analyze the energetic impact that the traffic volume migration of the U2100 band causes in the receiving bands, which will be determined through the mentioned energy consumption models. Fig. 7 presents the power consumption for the real data, measured before the traffic volume migration, as well as the predicted power consumption after the migration, estimated by the energy consumption models.

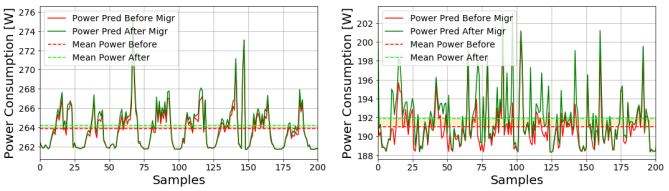

(a) For GU900 RRU. **(b)** For L800 (cell C) RRU.

Fig. 7: Comparison of power consumption before and after migration.

As expected, the traffic of U2100 that was migrated to the other bands, does not generate a high increase in the power consumed by the radios present in the current site and sector.

Thereby, a study of RRUs power consumption is developed, in order to estimate the energetic impact on the present site and sector due to the U2100 band switch-off. In Table III it is possible to analyze the difference between the real power consumption (pre-migration) and the expected power consumption (post-migration).

TABLE III: Balance of RRUs energy consumption.

	$P^{50\%}$ [W]		$P^{95\%}$ [W]		Avg Power [W]	
Band	**Before**	**After**	**Before**	**After**	**Before**	**After**
L800	190.47	191.28	195.63	197.26	191.02	191.85
U2100	212.33	0	220.89	0	213.69	0
GU900	263.56	263.87	267.32	268.04	263.88	264.21
TOTAL	**666.35**	**455.14**	**683.84**	**465.30**	**668.60**	**456.06**

The energy consumption balance, shown in Table III, presents some calculations regarding the power consumed by the RRUs of the current site and sector, such as power values in busy hour (95th percentile), median (50th percentile) and also mean power. Performing a deeper analysis at the level of the mean power, it is estimated an increase of 0.43% in the RRU that operates in the L800 band, corresponding to 0.83 W in energy consumption, and also an increase of 0.12% in the average power of the shared GU900 RRU, which corresponds to 0.33 W. On the other hand, there is a reduction of 100% in the overall power of the RRU operating in the U2100 band, since this one has been switched off. Therefore, a 31.79% reduction in the total average power consumed by all the RRUs of that site and sector is estimated, resulting in a decrease of 212.54 W.

VI. 3G Traffic Migration Scenario

A. Methodology

As already mentioned, in Europe, it is estimated that Mobile Network Operators (MNOs) will turn-off the 3G networks before 2G, which is primarily due to the extensive roll-out of Machine-to-Machine (M2M) and Internet of Things (IoT) types of services based on 2G technology. The cost of migrating a large number of M2M connections remains a cause for concern by the MNOs, being a key factor in maintaining 2G longer than 3G services [9]. Thus, the current scenario suggests a complete 3G shutdown, releasing both U900 and U2100 frequency bands by swapping their traffic to other technologies.

The purpose was to create a more complex scenario than the previous section, since the traffic migration will be based on the coverage areas mapping of each cell belonging to the site and sector, through the development of a link budget that approximately portrays the real radio propagation conditions of the cells in question. After the cell coverage mapping and subsequent traffic volume transfer, the BS energy consumption is analyzed using the models presented in Chapter 4 for RRUs that operate on a single technology. Thus, the study was carried out for a BS composed of radios separated by 82 frequency band, in order to be able to switch-off the U900 band RRU, which was not allowed in the previous scenario since the respective site owns radios shared between the G900 and U900 frequency bands.

B. Link Budget

This subsection comprises of a link budget for both uplink and downlink transmission directions held for the site and sector consisting of a G900 cell, one U900 cell, two U2100 cells and, finally, a cell for each 4G frequency band: L800, LTE 1800 MHz (L1800) and LTE 2600 MHz (L2600), already referred as cell D1, D2 and D3, respectively. The presented calculations as well as the typical values adopted during the link budget development are based on approaches detailed in [10] and [11].

In a first phase, the link budget calculations estimate the maximum allowed signal attenuation (path loss) between the mobile and the BS antenna. The maximum path loss allows the maximum cell range to be estimated with a suitable propagation model.

The link budget was built in parallel for each frequency band from the different network technologies, going into detail on 3G services (CS, PS R99 and High Speed Packet Access (HSPA)). In this subsection, link budget calculations are briefly discussed. Several parameters were obtained by manipulating the actual data from the respective cells, whenever possible, in order to obtain a more reliable estimate.

In order to portray the conditions observed at the cell edge, the data rate was given through the 5th percentile values of the user throughput measured in each cell. For the 3G technology data services, it was calculated the PS interactive High Speed (HS) and Dedicated Transport Channel (DCH) / Forward Access Channel (FACH) user throughput in both downlink and uplink directions, in a measurement period of 15 minutes, while the Adaptive Multi-Rate (AMR) 12.2 kbps bit rate was used for both 2G and 3G voice service. In the case of the LTE network, the 5th percentile of the L800 cell throughput was calculated, while for the remaining bands the user throughput was estimated based on the proportion of bandwidth relative to the L800 cell using its 5th percentile user throughput value. Since the L800 cell bandwidth is 10 MHz and, in turn, the bandwidth of both L1800 and L2600 cells is 20 MHz, the data rates of these last cells will be twice the 5th percentile of the first cell throughput.

Although the MNO provides BS maximum transmission power values, it was necessary to map the 3G power, since the link budget is held for the different services. The maximum transmit power, P_{Total}, which has to be divided by all the transport channels. With HSDPA, the total power is given by, [12]:

$$P_{Total} = P_{CCH} + P_{DCH} + P_{HSDPA} \quad (8)$$

where P_{CCH} is the power allocated to the control channels, P_{DCH} the power of DCH and P_{HSDPA} the power available for the service HSDPA.

Voice and PS R99 users are allocated on dedicated channels (DCH), which carry various services, such as AMR with different bit rates and the various PS R99 (8, 16, 32, 64, 128, 144, 256 and 384 kbps). Hence, a simple MLR model was developed, whose coefficients are used to estimate the respective powers, and it is described by:

$$P_{Total} = \beta_0 + \beta_1 R_{Voice} + \beta_2 R_{PS_{R99}} + \beta_3 R_{HSDPA}. \quad (9)$$

The independent variables are the normalized bit rates corresponding to the services of voice (R_{Voice}), PS R99 ($R_{PS_{R99}}$) and HSDPA (R_{HSDPA}), whose respective powers are given by P_{Voice}, $P_{PS_{R99}}$ and P_{HSDPA}. With the intercept and the coefficients of the independent variables, it is possible to estimate the proportion of power allocated to each transport channel. The intercept will represent the P_{CCH}, while the remaining coefficients will depict the power of the respective services. The approximate values of the proportions are: 17.5%, 23.1%, 2.4% and 57,0% for P_{CCH}, P_{Voice}, $P_{PS_{R99}}$ and P_{HSDPA}, respectively.

The LTE SINR value depends on the modulation and coding schemes, which again depend on the data rate and on the number of resource blocks allocated. The number of PRBs depends on the bandwidth. As mentioned, the downlink bandwidth is fixed by the MNO, while a 360 kHz uplink LTE bandwidth is assumed, which corresponds to an allocation of two PRBs [13]. Multiplying the data rate on cell edge (given by the 5$^{\text{th}}$ percentile of user throughput) by 1 ms, the Transport Block Size (TBS) value is obtained, since it represents the number of bits which can be transmitted per 1 Transmission Time Interval (TTI), which is 1 ms long. Giving the TBS value and the number of PRBs, the TBS index can be determined, leading further to the CQI value, which is then used to map SINR.

For UMTS SINR, the procedure was similar to the LTE approach. Once again, the TBS is the number of bits that can be transmitted per 1 TTI, which, in turn, is equal to 2 ms for UMTS. The TBS value can be calculated by multiplying the user throughput by 2 ms. Assuming the UE belong to Category 14 devices, while it uses 64-QAM and does not use MIMO, it is possible to map the CQI with the TBS value. Finally, the UMTS SINR can be given by, [14]:

$$CQI = SINR + 4.5. \quad (10)$$

A propagation model describes the average signal propagation and converts the maximum allowed propagation loss to the maximum cell range. It depends on conditions such as environment (urban, rural, etc), distance, frequency, indoor/outdoor and atmospheric conditions. One of the most widely used radio propagation estimate models is the Okumura-Hata model, especially in urban environments, and it is described in dB by, [15]:

$$\begin{aligned} L_U = 69.55 + 26.16\log_{10}(f) - 13.82\log_{10}(h_{BS}) - \\ -C_H + [44.9 - 6.55\log_{10}(h_{BS})]\log_{10}(d) \end{aligned} \quad (11)$$

where L_U is the pass loss in urban areas, f is the frequency of transmission in MHz, h_{BS} is the effective height of BS antenna in meters and d is the distance between BS and Mobile Station (MS) in km. In addition, C_H is a correction factor which depends on the environment type. For small and medium-sized cities it is given in dB by, [15]:

$$C_H = 0.8 + (1.1\log_{10}(f) - 0.7)h_{MS} - 1.56\log_{10}(f) \quad (12)$$

where h_{MS} is the height of MS antenna. For large cities and frequencies between 150 and 1500 MHz, the correction factor is presented in dB by, [15]:

$$C_H = \begin{cases} 8.29[\log_{10}(1.54h_{MS})]^2 - 1.1, & f \leq 200 \\ 3.2[\log_{10}(11.75h_{MS})]^2 - 4.97, & f \geq 400 \end{cases}. \quad (13)$$

In this scenario, the site is located in Lisbon, thus, considering its size, the correction factor for medium cities was used. The h_{MS} is assumed to be fixed to 1.5 meters [13], while the h_{BS} is provided by the MNO.

C. Migration and Capacity Analysis

With the development of the link budget for uplink and downlink it is observed that the distances between BS and MS are mostly more restrictive for uplink and, therefore, traffic volume will be transferred according to them. In order to map the traffic proportions to be transferred, the cell coverage areas, A_{Cell} in this direction of transmission are calculated by, [16]:

$$A_{Cell} = \frac{3\sqrt{3}}{2}R^2, \quad (14)$$

where R is the distance radius coverage given also by d.

In first place, the coverage area of UMTS voice service is smaller than the coverage area corresponding to the G900 cell, thus, the voice traffic volume of both U900 and U2100 cells is migrated to the G900 cell. In order to determine the UMTS voice traffic in Erlangs, ρ_{Voice}, which is firstly given by Mbps, (15) is used, where λ_m is the voice traffic in bps, given by Key Performance Indicators (KPIs), and μ_m is the several data rates available on voice services and, consequently, the channel capacity, also in bps, being $m = \{12, 64, \text{Adaptive Multi-Rate Wideband (AMR-WB)}\}$, allowing the voice traffic transfer from UMTS to GSM [17].

$$\rho_{Voice} = \sum \frac{\lambda_m}{\mu_m}. \quad (15)$$

In addiction, the coverage area of L2600 involves the areas corresponding to the U2100 data services (comprised of R99 and HSPA), thus their data traffic volume are transferred directly to the L2600 cell. However, the same does not happen with the U900 data services area, which is wider than the L2600 cell coverage area and, thus, traffic migration proportions are calculated for each 4G cell, based on the comparison of each cell area. Through the proportions mapping, 49.88% of the U900 data traffic volume is transferred to the L2600 cell, 33.19% to the L1800 cell and, finally, the remaining 16.93% are migrated to the L800 cell.

With migration, the G900 voice traffic volume rises to an average of 483.48%, after receiving the 3G voice traffic. In turn, the L2600 cell is the 4G cell that receives more data traffic from U900 cell while obtaining the entire U2100 data traffic, therefore, its traffic volume increases by an average of 91.79%, whereas the data traffic volume from L800 and L1800 cells increases 5.23% and 1.79%, respectively, after receiving the remaining U900 data traffic.

Fig. 8 shows the real PRB utilization rate as well as the estimated rate after the transfer, for L2600 cell (cell D3), during high traffic periods (for samples with cell throughput above the 70th percentile), using the PRB usage prediction model developed for the present cells, described in Section III, by adding the new traffic volume to the previous independent variable value of data traffic volume. Although the cell in question receives a significant amount of data traffic volume, it offers some capacity margin, since the PRB usage rate remains far from reaching 100% (maximum use of resources) with an increase of nearly 8.76% during the busy hour of the estimated period, confirming that the migration of data traffic does not negatively impact recipient cells.

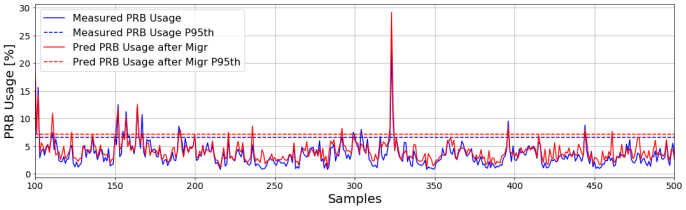

Fig. 8: 4G PRB usage prediction after traffic migration.

D. Energy Balance

Using the energy consumption models presented in Section II, an energy consumption balance is performed, analyzing the impact that the migration detailed above causes on the receiving cells. Fig. 9 displays the energy consumption for the measured traffic data along with the estimated energy consumption after the migration, both predicted using the RRUs power consumption models, for G900 and L2600 RRUs, once the latter receives more traffic volume than the other 4G cells.

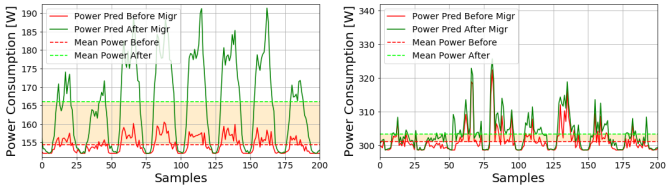

(a) For G900 RRU. **(b)** For L2600 (cell D3) RRU.

Fig. 9: Comparison of power consumption before and after migration.

Since the majority of power consumption is baseline, it is expected that the increase in traffic on the radios that remain on will not have a significant impact on their energy consumption. To prove this statement, an analysis of RRUs power consumption is conducted for the radios present in the current site and sector, thus studying the energy impact generated by the switch-off of 3G RRUs. Table IV details a comparison between the energy consumption before and after the traffic volume transfer. The study does not include the power consumption of the remaining BS components.

TABLE IV: Balance of RRUs energy consumption.

	$P^{50\%}$ [W]		$P^{95\%}$ [W]		Avg Power [W]	
Band	**Before**	**After**	**Before**	**After**	**Before**	**After**
L2600	300.29	302.65	306.45	311.41	301.11	303.39
L1800	289.73	290.05	310.18	311.07	289.51	289.88
L800	188.83	189.07	195.85	196.06	189.63	189.82
U2100	165.68	0	169.87	0	166.03	0
U900	155.48	0	162.89	0	155.65	0
G900	153.94	165.01	158.44	185.23	154.40	166.02
TOTAL	**1253.94**	**946.78**	**1303.68**	**1003.77**	**1256.33**	**949.11**

The balance of power consumption, presented in Table IV, provides several estimates of the power consumed by each RRU in different circumstances such as power values in busy hour (95th percentile), median (50th percentile) and also average power. Regarding the mean values, the L800, L1800 and L2600 RRUs suffer an increase of 0.10%, 0.13% and 0.75% in power consumption, which corresponds to 0.19 W, 0.37 W and 2.27 W, respectively, whereas G900 RRU power consumption increases 7.53%, corresponding to 11.63 W. Nevertheless, the energy consumption of both 3G RRUs is reduced by 100% with their switch-off. Thus, a reduction of 24.45% is finally obtained in the total average power consumed by all the radios belonging to the current site and sector, leading to a global decrease of 307.23 W.

VII. 5G Hypothetical Migration Scenario

A simple migration scenario was created for the current data, consisting of data traffic volume migration from 4G to 5G, considering the worst possible scenario; in this case, even though the cell coverage of 5G is much smaller than the cell coverage of 4G, the total volume of data traffic from the 4G cell, belonging to the same site and sector, was transferred to the current 5G cell. The data traffic migration results are presented in Fig. 10.

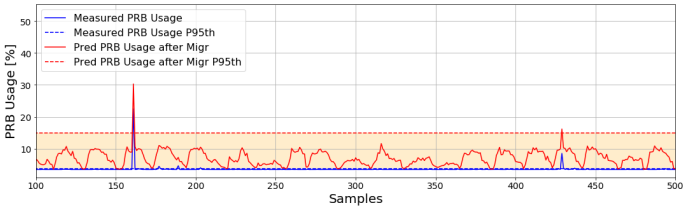

Fig. 10: 5G PRB usage prediction after traffic migration.

As shown in Fig. 10, the calculated 95th percentile value of measured PRB utilization rate is 3.70%, since 5G only

presents residual traffic volume as mentioned. On the other hand, for the estimated PRB utilization rate after migration, the calculated 95$^{\text{th}}$ percentile value is 14.99%; therefore, it can then be concluded that the current 5G cell has sufficient resources to receive the 4G mobile data traffic volume.

VIII. Conclusions

This paper presents cell capacity prediction models, in downlink direction, for both 4G and 5G technologies, using MLR algorithms, along with traffic volume migration scenarios using existing energy consumption models.

The LTE model consists of two modules, one where cells with capacity saturation were detected and another where the downlink cell throughput was predicted with a R_a^2 of 0.991, which corroborates the high reliability of the model along with the other error metrics provided. It is then estimated the maximum cell capacity for the cell radio propagation environment using the proposed MLR model to calculate the maximum cell throughput, by setting the PRB utilization rate to 100%. At the busy hour, the cell present almost no capacity margin, resulting in a cell load of 97.46%, demonstrating that it is approaching an overload situation.

An additional 4G model was developed estimating downlink PRB utilization rate, which can be used to validate or not the traffic migration scenarios performed for this vendor, presenting a R_a^2 of 0.964. Thus, two traffic migration scenarios were developed for these cells: the first is based on the U2100 frequency band switch-off, while the second one is more complex since it performs the complete 3G switch-off including the development of a link budget for both uplink and downlink. Within the U2100 traffic migration scenario, the corresponding traffic transfers generated a 31.79% reduction in the total average power consumed by all the RRUs of that site and sector, resulting in a decrease of 212.54 W. Regarding the 3G traffic migration scenario, the transfer was based on the coverage areas mapping, through the development of a link budget that approximately portrays the real radio propagation conditions of the cells in question. Once more, the energy consumption balance was performed resulting in a reduction of 24.45% in the total average power consumed by all the radios belonging to the current site and sector, leading to a global decrease of 307.23 W.

Finally, a 5G cell resource prediction model has been proposed, with a R_a^2 of 0.948, despite the predominance of residual traffic in the measured data that were used in the model development. Additionally, a simple scenario of data traffic volume migration from a 4G cell to a 5G cell was created in order to predict the impact of 4G traffic on the resources that 5G provides, concluding that 5G technology has sufficient cell resources.

Acknowledgment

The author would like to thank "Instituto de Telecomunicações" (IT) and CELFINET for supporting this work.

References

[1] Ericsson. "Ericsson Mobily Report", Tech. Rep., June 2020. [Online]. Available: https://www.ericsson.com/49da93/assets/local/mobility-report/documents/2020/june2020-ericsson-mobility-report.pdf.

[2] J. A. Fernández-Segovia, S. Luna-Ramírez, M. Toril and J. J. Sánchez-Sánchez, "Estimating Cell Capacity From Network Measurements in a Multi-Service LTE System", *IEEE Communications Letters*, vol. 19, no. 3, pp. 431-434, March 2015.

[3] M. H. Alsharif, R. Nordin, and M. Ismail, "Survey of Green Radio Communications Networks: Techniques and Recent Advances", *Journal of Computer Networks and Communications*, 2013.

[4] T. Saraiva, D. Duarte, I. Pinto and P. Vieira, "An Improved BBU/RRU Energy Consumption Predictor for 4G and Legacy Mobile Networks using Mixed Statistical Models", *2020 International Conference on Computing, Networking and Communications (ICNC)*, Big Island, HI, USA, pp. 320-325, 2020.

[5] D. Parracho, D. Duarte, I. Pinto and P. Vieira, "An Improved Capacity Model based on Radio Measurements for a 4G and beyond Wireless Network", *2018 21st International Symposium on Wireless Personal Multimedia Communications (WPMC)*, Chiang Rai, Thailand, pp. 314-318, 2018.

[6] Huawei, "eRAN Capacity Monitoring Guide", Huawei Technologies Co., Ltd., 2016.

[7] Ericsson Internal, "LTE Post Launch Optimization Problem Cause, Counter Pegging, Solution & Case Study", Ericsson AB, 2016.

[8] D. Montgomery and G. Runger, *Applied Statistics and Probability for Engineers*, John Wiley and Sons, 2003.

[9] GSMA, "Legacy Mobile Network Rationalisation," April 2020.

[10] A. T. Harri Holma, *WCDMA for UMTS: HSPA evolution and LTE*, 4th ed. Wiley, 2007.

[11] A. T. Harri Holma, *LTE for UMTS - OFDMA and SC-FDMA Based Radio Access*, 1st ed. Wiley, 2009.

[12] P. Zanier and D. Soldani, "A simple approach to HSDPA dimensioning," in *2005 IEEE 16th International Symposium on Personal, Indoor and Mobile Radio Communications*, vol. 2, September 2005, pp. 883–887.

[13] A. T. Harri Holma, *WCDMA for UMTS: HSPA evolution and LTE*, 4th ed. Wiley, 2007.

[14] C. Kurnaz, B. K. Engiz, and M. O. Esenalp, "Challenges and Enabling Technologies for Energy Aware Mobile Radio Network," *Turkish Journal of Electrical Engineering & Computer Sciences*, November 2017.

[15] J. T. J. Penttinen, *The Telecommunications Handbook: Engineering Guidelines for Fixed, Mobile and Satellite Systems*, 1st ed. John Wiley and Sons, 2015.

[16] F. Richter, A. J. Fehske, and G. P. Fettweis, "Energy Efficiency Aspects of Base Station Deployment Strategies for Cellular Networks," in 2009 *IEEE 70th Vehicular Technology Conference Fall*, 2009, pp. 1–5.

[17] P. A. García, A. A. González, A. A. Alonso, B. C. Martínez, J. M. A. Pérez, and A. S. Esguevillas, "Automatic UMTS system resource dimensioning based on service traffic analysis," *EURASIP Journal on Wireless Communications and Networking*, October 2012.